

# Lack of Microsomal Prostaglandin E<sub>2</sub> Synthase-1 in Bone Marrow-Derived Myeloid Cells Impairs Left Ventricular Function and Increases Mortality After Acute Myocardial Infarction

Norbert Degousee, PhD\*; Jeremy Simpson, PhD\*; Shafie Fazel, MD, PhD\*†; Klaus Scholich, PhD\*; Denis Angoulvant, MD, PhD; Carlo Angioni, BSc; Helmut Schmidt, PhD†; Marina Korotkova, MD, PhD; Eva Stefanski, MSc; Xing-Hua Wang, MD; Thomas F. Lindsay, MD, MSc; Efrat Ofek, MD; Sandra Pierre, PhD; Jagdish Butany, MBBS, MS; Per-Johan Jakobsson, MD, PhD; Armand Keating, MD; Ren-Ke Li, MD, PhD; Matthias Nahrendorf, MD, PhD; Gerd Geisslinger, MD, PhD; Peter H. Backx, PhD; Barry B. Rubin, MD, PhD

**Background**—Microsomal prostaglandin E<sub>2</sub> synthase-1 (mPGES-1), encoded by the *Ptges* gene, catalyzes prostaglandin E<sub>2</sub> biosynthesis and is expressed by leukocytes, cardiac myocytes, and cardiac fibroblasts. *Ptges*<sup>-/-</sup> mice develop more left ventricle (LV) dilation, worse LV contractile function, and higher LV end-diastolic pressure than *Ptges*<sup>+/+</sup> mice after myocardial infarction. In this study, we define the role of mPGES-1 in bone marrow-derived leukocytes in the recovery of LV function after coronary ligation.

**Methods and Results**—Cardiac structure and function in *Ptges*<sup>+/+</sup> mice with *Ptges*<sup>+/+</sup> bone marrow (*BM*<sup>+/+</sup>) and *Ptges*<sup>+/+</sup> mice with *Ptges*<sup>-/-</sup> BM (*BM*<sup>-/-</sup>) were assessed by morphometric analysis, echocardiography, and invasive hemodynamics before and 7 and 28 days after myocardial infarction. Prostaglandin levels and prostaglandin biosynthetic enzyme gene expression were measured by liquid chromatography–tandem mass spectrometry and real-time polymerase chain reaction, immunoblotting, immunohistochemistry, and immunofluorescence microscopy, respectively. After myocardial infarction, *BM*<sup>-/-</sup> mice had more LV dilation, worse LV systolic and diastolic function, higher LV end-diastolic pressure, more cardiomyocyte hypertrophy, and higher mortality but similar infarct size and pulmonary edema compared with *BM*<sup>+/+</sup> mice. *BM*<sup>-/-</sup> mice also had higher levels of COX-1 protein and more leukocytes in the infarct, but not the viable LV, than *BM*<sup>+/+</sup> mice. Levels of prostaglandin E<sub>2</sub> were higher in the infarct and viable myocardium of *BM*<sup>-/-</sup> mice than in *BM*<sup>+/+</sup> mice.

**Conclusions**—Lack of mPGES-1 in bone marrow-derived leukocytes negatively regulates COX-1 expression, prostaglandin E<sub>2</sub> biosynthesis, and inflammation in the infarct and leads to impaired LV function, adverse LV remodeling, and decreased survival after acute myocardial infarction. (*Circulation*. 2012;125:2904-2913.)

**Key Words:** leukocytes ■ myocardial infarction ■ prostaglandins ■ remodeling ■ chimeric mice

Ischemic heart disease and myocardial infarction (MI) will be the leading cause of death worldwide by 2020.<sup>1</sup> MI leads to an inflammatory response characterized by the generation of proinflammatory mediators and the influx of leukocytes that are necessary to remove necrotic cellular debris and promote recovery of left ventricular (LV) contractile function. An improperly regulated inflammatory response

and pathological LV remodeling can impair LV function and lead to heart failure and death after MI.<sup>2,3</sup>

## Editorial see p 2818 Clinical Perspective on p 2913

Prostaglandins, synthesized by the sequential action of phospholipase A<sub>2</sub> (PLA<sub>2</sub>), cyclooxygenases (COX-1 and/or

Received November 28, 2011; accepted April 4, 2012.

From the Divisions of Vascular Surgery (N.D., E.S., T.F.L., B.B.R.), Cardiac Surgery (S.F., R.-K.L.), Cardiology (P.H.B.), and Pathology (E.O., J.B.), Peter Munk Cardiac Centre, and the Department of Medical Oncology & Hematology (X.-H.W., A.K.), Toronto General Hospital, University Health Network, Toronto, Canada; Departments of Physiology and Medicine, University of Toronto, Toronto, Ontario, Canada (J.S., P.H.B.); Institut für Klinische Pharmakologie, Frankfurt am Main, Germany (K.S., C.A., H.S., S.P., G.G.); Division of Cardiology, Trousseau Hospital, Tours University Hospital Center and EA 4245, François Rabelais University, Tours, France (D.A.); Department of Medicine, Rheumatology Unit, Karolinska University Hospital, Stockholm, Sweden (M.K., P.-J.J.); and Center for Systems Biology, Massachusetts General Hospital and Harvard Medical School, Boston, MA (M.N.).

†Deceased.

\*Drs Degousee, Simpson, Fazel, and Scholich contributed equally to this article.

The online-only Data Supplement is available with this article at <http://circ.ahajournals.org/lookup/suppl/doi:10.1161/CIRCULATIONAHA.112.099754/-/DC1>.

Correspondence to Barry B. Rubin, MD, PhD, Medical Director, Peter Munk Cardiac Centre, Division of Vascular Surgery, University Health Network, 200 Elizabeth St, EN6-222, Toronto, Ontario, Canada M5G-2C4. E-mail [barry.rubin@uhn.on.ca](mailto:barry.rubin@uhn.on.ca)

© 2012 American Heart Association, Inc.

*Circulation* is available at <http://circ.ahajournals.org>

DOI: 10.1161/CIRCULATIONAHA.112.099754

COX-2), and terminal prostaglandin synthase enzymes, participate in the regulation of the inflammatory response after MI. Prostaglandin E<sub>2</sub> (PGE<sub>2</sub>) is the principal prostaglandin generated by cardiac myocytes.<sup>4</sup> The terminal step in PGE<sub>2</sub> biosynthesis may be catalyzed by the constitutively expressed enzymes cytosolic or microsomal PGE<sub>2</sub> synthase-2 (cPGES and mPGES-2, respectively),<sup>5</sup> or by mPGES-1, an inducible enzyme. mPGES-1 is encoded by the *Ptges* gene and can be expressed by leukocytes,<sup>7</sup> cardiac fibroblasts,<sup>8</sup> and cardiac myocytes.<sup>9</sup>

Inhibition of the PGE<sub>2</sub> receptor EP4 attenuates cardiomyocyte hypertrophy in vitro,<sup>10</sup> and deletion of EP4 exacerbates myocardial ischemia/reperfusion injury in vivo.<sup>11</sup> In addition, *Ptges*<sup>-/-</sup> mice develop more LV dilation, worse LV contractile function, and higher LV end-diastolic pressure than *Ptges*<sup>+/+</sup> mice after MI.<sup>12</sup> Collectively, these observations suggest a beneficial role for mPGES-1-mediated PGE<sub>2</sub> biosynthesis in postinfarction LV remodeling. The cellular source of mPGES-1 in the heart after MI has not been identified. In this study, we show that deletion of mPGES-1 in bone marrow-derived leukocytes results in a more intense inflammatory response, pathological LV remodeling, and increased mortality after acute MI in vivo.

## Methods

Reagents were from Sigma Chemical Co (St. Louis, MO) unless otherwise stated. Construction of the mPGES-1-deficient mouse line (*Ptges*<sup>-/-</sup>, DBA/11acJ background),<sup>13</sup> real-time quantitative polymerase chain reaction studies, 2-dimensional echocardiography, invasive hemodynamic assessment of LV function, morphometric assessment of hearts that were perfusion fixed at an intraventricular pressure of 20 mm Hg in situ, liquid chromatography-tandem mass spectrometry-based evaluation of prostanoid levels in cardiac tissue, immunoblotting, and lectin and Picrosirius Red staining were performed exactly as described previously.<sup>9,12,14</sup> Housing and experimental procedures were approved by the Animal Care Committee of the University Health Network and were in accordance with the *Guide for the Care and Use of Laboratory Animals* research statutes, Ontario (1980).

## MI Model

Mice were sedated with ketamine (50 mg/kg) and xylazine (5 mg/kg), intubated, ventilated, and maintained with 2% isoflurane. Through a left thoracotomy, the left coronary artery was ligated 1 to 2 mm below the border of the left atrial appendage. Ischemia was confirmed by the appearance of hypokinesia and pallor distal to the occlusion and by ST elevation on ECG.<sup>12</sup>

## Multiple Epitope Ligand Cartography

Multiple epitope ligand cartography was performed as described previously.<sup>15</sup> Briefly, a slide with a cardiac section was placed on the stage of an inverted wide-field fluorescence microscope (Leica DM IRE2). By an automated process, tissue slices were incubated for 15 minutes with a fluorescence-labeled antibody and rinsed with wash solution, and fluorescence signals were imaged. A bleaching step was then performed to delete the fluorescence signal before addition of the next antibody. Postbleaching images were recorded and subtracted from the following fluorescence image.

Bone marrow transplantation and the generation of chimeric mice, isolation and coculture of cardiac fibroblasts and bone marrow-derived mononuclear cells/macrophages, antisera for immunohistochemistry, primer sequences for real-time reverse-transcription polymerase chain reaction analysis, and the statistical analysis appear in the online-only Data Supplement.

The authors had full access to and take full responsibility for the integrity of the data. All authors have read and agree to the manuscript as written.

## Results

### LV Dilation, Impaired LV Systolic and Diastolic Function, and Increased Mortality After MI in Mice That Lack mPGES-1 in Bone Marrow-Derived Cells

To define the role of mPGES-1 in myeloid cells in the pathophysiology of acute MI, we generated chimeric *Ptges*<sup>+/+</sup> mice with *Ptges*<sup>+/+</sup> bone marrow (*BM*<sup>+/+</sup>) and *Ptges*<sup>+/+</sup> mice with *Ptges*<sup>-/-</sup> bone marrow (*BM*<sup>-/-</sup>) and evaluated cardiac dimensions and function in these mice before (t=0) and up to 28 days after coronary ligation. Bone marrow cells in chimeras were predominantly from donor mice before and up to 28 days after MI (Figure 1A). After MI, survival was significantly worse in *BM*<sup>-/-</sup> than in *BM*<sup>+/+</sup> mice, and most deaths occurred between 19 and 28 days after infarction (Figure 1B). At 28 days post-MI, LV volume (Figures 1C and 1D) and diameter (Table), measured after hyperkalemic arrest and constant-pressure in situ perfusion fixation,<sup>12</sup> were 43% and 30% greater in *BM*<sup>-/-</sup> than *BM*<sup>+/+</sup> mice, respectively. Conversely, the volume of infarcted myocardium (Figures 1C and 1E) and the thickness of the interventricular septum (Table) were similar in *BM*<sup>+/+</sup> and *BM*<sup>-/-</sup> mice 28 days after MI.

Next, we assessed LV dimensions and LV function in *BM*<sup>+/+</sup> and *BM*<sup>-/-</sup> chimeras in vivo by 2-dimensional echocardiography and invasive hemodynamic monitoring. The decrease in LV fractional shortening in *BM*<sup>+/+</sup> and *BM*<sup>-/-</sup> mice 7 days after coronary ligation was comparable and indicated significant MI in both groups of mice (Figure 1F). Fractional shortening and +dP/dt (Figure 1G), indexes of LV systolic function, and -dP/dt and  $\tau$  (Figures 1H and 1I), indicators of the diastolic properties of the LV, were all significantly worse in *BM*<sup>-/-</sup> than *BM*<sup>+/+</sup> mice 28 days after MI. *BM*<sup>-/-</sup> mice also had higher LV diameter and LV volume at end systole but not end diastole, a lower stroke volume (Table), and higher LV end-diastolic pressure (Figure 1J) than *BM*<sup>+/+</sup> mice 28 days after MI. Collectively, these findings established accelerated deterioration of cardiac function in *BM*<sup>-/-</sup> compared with *BM*<sup>+/+</sup> chimeras after MI. Although stroke volume and cardiac output in *BM*<sup>+/+</sup> mice recovered by 28 days after MI to baseline levels, possibly reflecting compensatory remodeling (Table), fractional shortening, stroke volume, and cardiac output remained below baseline levels in *BM*<sup>-/-</sup> mice (Figure 1F; Table) 28 days after MI.

The surface area of cardiac myocytes, a measure of cardiomyocyte hypertrophy,<sup>12</sup> increased more in *BM*<sup>-/-</sup> than *BM*<sup>+/+</sup> mice 28 days after MI (Figures 1L and 1M). Despite differences in cardiomyocyte hypertrophy and cardiac function, respiratory rate (Table) and the pulmonary wet-to-dry weight ratio (Figure 1K) were similar in *BM*<sup>+/+</sup> and *BM*<sup>-/-</sup> mice after MI. In addition, there was no difference in collagen remodeling (Figures 1N and 1O), matrix metalloproteinase-2 or -9 mRNA expression (online-only Data Supplement Figure 1), endothelial cell growth (CD31; online-only Data Supple-

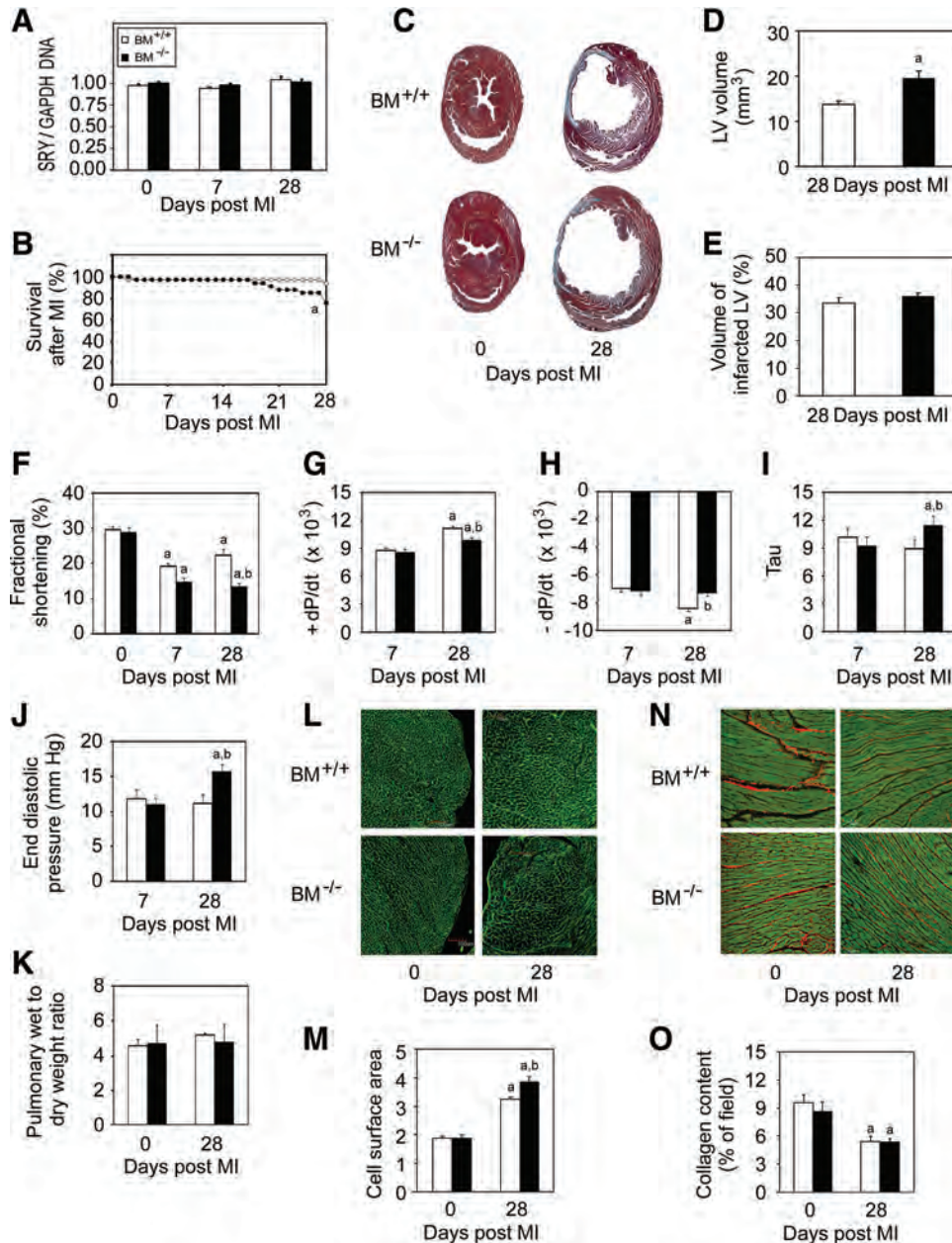


**Figure 1.** Lack of microsomal prostaglandin E<sub>2</sub> synthase-1 (mPGES-1) in myeloid cells leads to adverse left ventricular (LV) remodeling and decreased survival after myocardial infarction (MI). **A**, Ratio of SRY/GAPDH DNA after MI in bone marrow (BM) cells after irradiation of female *Ptges*<sup>+/+</sup> mice and transplantation with BM from male *Ptges*<sup>+/+</sup> (*BM*<sup>+/+</sup>; open bars) or *Ptges*<sup>-/-</sup> mice (*BM*<sup>-/-</sup>; solid bars). **B**, Survival of *BM*<sup>+/+</sup> and *BM*<sup>-/-</sup> mice after MI ( $P=0.04$ , log-rank test). **C**, Masson's trichrome staining of explanted hearts after hyperkalemic arrest and perfusion fixation in situ at physiological pressure. **D**, LV volume; **E**, volume of infarcted myocardium; **F**, fractional shortening; **G**, +dP/dt; **H**, -dP/dt; **I**,  $\tau$ ; and **J**, LV end-diastolic pressure. Invasive hemodynamic assessment of LV function at baseline ( $t=0$ ) was not possible, because the catheter was too large to fit in the LV before infarction. **K**, Pulmonary wet to dry weight ratio. **L** and **M**, Lectin stain (**L**) and cardiomyocyte surface area (**M**). **N** and **O**, Picosirius Red stain (**N**) and collagen content (**O**). Open circles or bars indicate *BM*<sup>+/+</sup> mice; solid circles or bars, *BM*<sup>-/-</sup> mice. a,  $P<0.05$  baseline vs 7 or 28 days after MI; b,  $P<0.05$ , *BM*<sup>-/-</sup> vs *BM*<sup>+/+</sup> mice at any time point. Data represent  $\geq 9$  independent experiments for each group.

ment Figure II), or myofibroblast formation (smooth muscle  $\alpha$ -actin; online-only Data Supplement Figure III) between *BM*<sup>+/+</sup> and *BM*<sup>-/-</sup> mice after MI.

Taken together, these results provide direct evidence that loss of mPGES-1 in bone marrow-derived myeloid cells leads to impaired LV systolic and diastolic function and is associated with increased mortality after coronary occlusion. Compared with *BM*<sup>+/+</sup> mice, *BM*<sup>-/-</sup> mice that survived 28 days after MI had impending LV failure,

manifested as LV dilation and an increase in LV end-diastolic pressure, but did not develop overt pulmonary edema. Because a lack of mPGES-1 in bone marrow-derived myeloid cells has no effect on infarct volume after coronary ligation but increases LV volume, LV end-diastolic pressure, and cardiomyocyte hypertrophy, these data are consistent with the notion that lack of mPGES-1 in bone marrow-derived myeloid cells impairs LV remodeling 28 days after MI in these mice.

**Table. Cardiac Dimensions and Function Before and 7 and 28 Days After Left Coronary Artery Ligation**

	Days After Coronary Ligation					
	0		7		28	
	<i>BM</i> <sup>+/+</sup> (n=14)	<i>BM</i> <sup>-/-</sup> (n=13)	<i>BM</i> <sup>+/+</sup> (n=13)	<i>BM</i> <sup>-/-</sup> (n=11)	<i>BM</i> <sup>+/+</sup> (n=10)	<i>BM</i> <sup>-/-</sup> (n=8)
LV diameter, end systole, mm‡	2.5±0.05	2.6±0.07	3.2±0.06*	3.3±0.1*	3.1±0.1*	3.6±0.07*†
LV diameter, end diastole, mm‡	3.6±0.04	3.7±0.06	3.9±0.06*	3.9±0.09	4.0±0.09*	4.1±0.07*
LV volume, end systole, μL‡	22±1.1	26±2.0	40±1.9*	45±3.1*	38±3.4*	53±2.8*†
LV volume, end diastole, μL‡	54±1.6	58±2.7	66±2.7*	66±3.6	69±3.7*	74±2.9*
Stroke volume, μL‡	31±0.9	33±1.8	26±1.4	21±1.9*	31±2.4	21±1.4*†
Cardiac output, mL/min‡	15±0.6	16±0.8	13±0.5*	11±1.1*	17±1.2	11±0.7*†
Heart rate, bpm‡	491±9	491±15	490±11	533±13	542±14	541±23
LV volume, μL§	ND	ND	ND	ND	13.7±0.7	19.6±1.6†
LV diameter, mm§	ND	ND	ND	ND	1.9±0.1	2.5±0.1†
Interventricular septum, mm§	ND	ND	ND	ND	1.4±0.1	1.3±0.1
Respiratory rate, breaths/min	ND	ND	163±11	165±7	158±9	139±9

BM indicates bone marrow; LV, left ventricular; and ND, not determined.

\**P*<0.05, 0 vs 7 or 28 d post-MI.

†*P*<0.05, *BM*<sup>+/+</sup> vs *BM*<sup>-/-</sup> mice.

‡In vivo 2-dimensional echocardiography.

§Ex vivo morphometric analysis.

Two-way ANOVA, followed by paired *t* tests, 2-tailed, unequal variance. Data represent ≥9 independent experiments for each group.

### Lack of mPGES-1 in Bone Marrow-Derived Cells Increases the Inflammatory Response to MI

MI stimulates an inflammatory response that is characterized by an increase in cytokine and chemokine gene expression and leukocyte recruitment to the heart. An appropriately regulated inflammatory response is necessary for physiological LV remodeling and healing after MI.<sup>16,17</sup> To assess the role of mPGES-1 in bone marrow-derived cells in the inflammatory response to MI, we studied the expression of a panel of genes that regulate inflammation in *BM*<sup>+/+</sup> and *BM*<sup>-/-</sup> mice. Levels of interleukin-1β (IL-1β), IL-1β receptor antagonist, and tumor necrosis factor-α mRNA in the infarct region increased significantly after MI in both chimeras, and the expression of these genes was higher in *BM*<sup>-/-</sup> than *BM*<sup>+/+</sup> mice 7 days after MI (Figures 2A through 2C). Levels of monocyte chemoattractant protein-1 and macrophage inflammatory protein-2 mRNA in the infarct also increased after MI in both chimeras but were not different between *BM*<sup>-/-</sup> and *BM*<sup>+/+</sup> mice (Figures 2D and 2E). Changes in keratinocyte-derived chemokine mRNA expression in the infarct were not identified after MI in these mice (Figure 2F). There was no difference in the expression of IL-1β, IL-1β receptor antagonist, tumor necrosis factor-α, monocyte chemoattractant protein-1, macrophage inflammatory protein-2, or keratinocyte-derived chemokine in the LV remote from the infarct between *BM*<sup>-/-</sup> and *BM*<sup>+/+</sup> mice (online-only Data Supplement Figure IV).

Next, we measured tissue levels of myeloperoxidase (MPO), an enzyme contained in the granules of neutrophils and monocytes that is released on leukocyte activation and that has been used as a marker of leukocyte infiltration into the heart after MI.<sup>16,17</sup> Levels of MPO were significantly higher in the infarct of *BM*<sup>-/-</sup> than *BM*<sup>+/+</sup> mice 7 but not 28

days after MI (Figures 2G and 2H). Conversely, there was no difference in MPO protein levels in the LV remote from the infarct between *BM*<sup>-/-</sup> and *BM*<sup>+/+</sup> mice after coronary ligation (online-only Data Supplement Figure IV).

To independently confirm the observation that leukocyte infiltration was augmented in the infarct of mice that lacked mPGES-1 in bone marrow-derived cells, we performed immunohistochemical analysis of CD45, which is expressed on leukocytes, and MPO before and 7 and 28 days after MI. Consistent with the results of the MPO immunoblotting studies, we found that levels of both CD45 (Figures 2I and 2J) and MPO (online-only Data Supplement Figure V) were significantly higher in the infarct of *BM*<sup>-/-</sup> than *BM*<sup>+/+</sup> mice 7 but not 28 days after MI. Taken together, these results demonstrate that lack of mPGES-1 in bone marrow-derived cells increases the inflammatory response to MI.

### Increased LV COX-1 Expression and Prostaglandin Levels in *BM*<sup>-/-</sup> Mice After MI

Targeted deletion of mPGES-1 leads to alterations in the biosynthesis of multiple prostaglandins in macrophages,<sup>7</sup> and macrophages are the most prominent inflammatory cells in the infarct zone 7 days after MI.<sup>18</sup> To explore whether changes in prostaglandin concentrations may explain the differences in leukocyte recruitment between *BM*<sup>-/-</sup> and *BM*<sup>+/+</sup> mice after coronary ligation, we measured levels of prostaglandins in the infarct zone and in the viable portion of the LV adjacent to the infarct by liquid chromatography-tandem mass spectrometry. Concentrations of PGE<sub>2</sub>, thromboxane B<sub>2</sub> (TxB<sub>2</sub>, a stable TxA<sub>2</sub> metabolite), PGF<sub>2α</sub>, 6 keto-PGF<sub>1α</sub> (a stable PGI<sub>2</sub> metabolite), and total prostaglandins were significantly higher in the infarct of *BM*<sup>-/-</sup> than

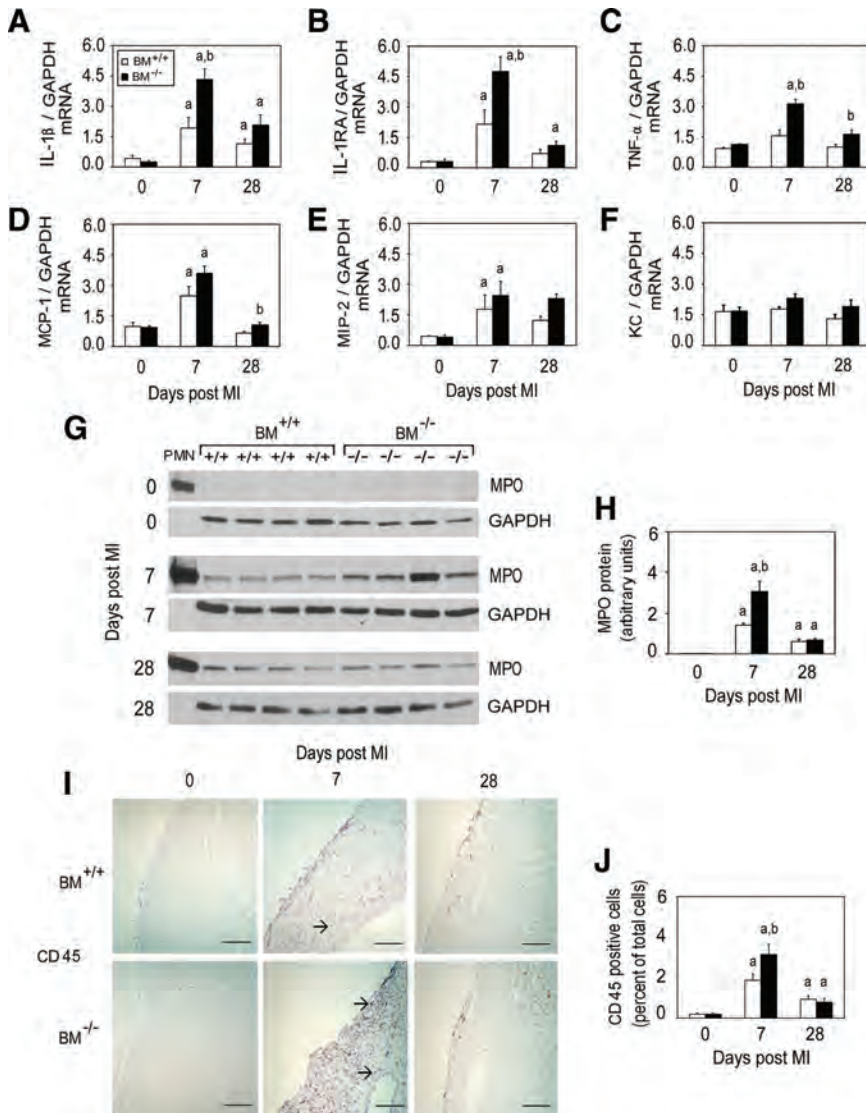


**Figure 2.** Lack of microsomal prostaglandin E<sub>2</sub> synthase-1 (mPGES-1) in bone marrow (BM)-derived cells increases the inflammatory response to myocardial infarction (MI). Ratio of interleukin-1β (IL-1β; **A**), IL-1β receptor antagonist (**B**), tumor necrosis factor-α (TNF-α; **C**), monocyte chemoattractant protein-1 (MCP-1; **D**), macrophage inflammatory protein-2 (MIP-2; **E**), and keratinocyte-derived chemokine (KC; **F**) to GAPDH mRNA before and 7 and 28 days after MI in the infarct. **G**, Representative immunoblot analysis of myeloperoxidase (MPO) and GAPDH protein from 4 *BM*<sup>+/+</sup> and *BM*<sup>-/-</sup> mice. **H**, Densitometric analysis of the ratio of MPO to GAPDH protein. **I**, Immunohistochemical analysis of CD45 before and 7 and 28 days after MI (magnification ×200). **J**, Percentage of CD45-positive cells per high-power field (indicated by arrow) before and 7 and 28 days after MI. Open bars indicate *BM*<sup>+/+</sup> mice; solid bars, *BM*<sup>-/-</sup> mice. a, *P*<0.05 baseline vs 7 or 28 days after MI, *BM*<sup>+/+</sup> or *BM*<sup>-/-</sup> mice; b, *P*<0.05, *BM*<sup>+/+</sup> vs *BM*<sup>-/-</sup> mice at any time point. Scale bars indicate 100 μm. Data represent ≥6 independent experiments for each group.

*BM*<sup>+/+</sup> mice 7 but not 28 days after MI (Figures 3A through 3F). Similarly, PGE<sub>2</sub>, PGD<sub>2</sub>, TxB<sub>2</sub>, 6 keto-PGF<sub>1α</sub>, and total prostaglandin levels were higher in the viable myocardium adjacent to the infarct in *BM*<sup>-/-</sup> than in *BM*<sup>+/+</sup> mice 7 but not 28 days after coronary ligation (online-only Data Supplement Figure VI, A through F).

To identify the molecular mechanisms that resulted in increased prostaglandin levels in the infarct and LV of *BM*<sup>-/-</sup> compared with *BM*<sup>+/+</sup> mice, we assessed prostaglandin biosynthetic enzyme gene expression in these chimeras after MI. Our studies focused on COX-1 and COX-2 because these enzymes catalyze the formation of PGH<sub>2</sub>, the precursor of all prostaglandins, and we noted an increase in the level of multiple prostaglandins after MI (Figure 3; online-only Data Supplement Figure VI). mRNA levels of COX-1, a constitutively expressed enzyme, and COX-2, an inducible enzyme, were higher in the infarct zone of *BM*<sup>-/-</sup> than *BM*<sup>+/+</sup> mice 7 and 28 days after MI (Figures 3G and 3H). The level of mPGES-1 mRNA in the infarct was also higher in *BM*<sup>-/-</sup> than *BM*<sup>+/+</sup> mice 7 but not 28 days after MI (Figure 3I). The source of the increase in mPGES-1 mRNA in the infarct of

*BM*<sup>-/-</sup> mice must have been resident cardiac cells, because bone marrow-derived cells recruited to the heart in these mice were from *Ptges*<sup>-/-</sup> mice (Figure 1A), which do not express mPGES-1 mRNA. There was no change in mPGES-2 mRNA levels in either chimera 7 or 28 days after coronary ligation (data not shown).

COX-1 protein levels in the infarct were higher in *BM*<sup>-/-</sup> than in *BM*<sup>+/+</sup> mice 7 but not 28 days after MI (Figures 3J and 3K). Conversely, the level of COX-2 protein in the infarct was higher in both *BM*<sup>+/+</sup> and *BM*<sup>-/-</sup> mice 7 and 28 days after coronary ligation than at baseline, but there was no difference in the level of COX-2 protein in the infarct between these chimeras after MI (Figures 3J and 3L). No change in the level of mPGES-1 (Figure 3M) or mPGES-2 protein (not shown) in the infarct of *BM*<sup>+/+</sup> or *BM*<sup>-/-</sup> mice was identified by immunoblot analysis. These data demonstrate that the loss of mPGES-1 in bone marrow-derived myeloid cells led to a compensatory increase in COX-1 protein expression in the infarcted myocardium after coronary ligation in *BM*<sup>-/-</sup> mice.

Next, we performed immunohistochemical analysis of cardiac sections to localize COX-1, COX-2, and mPGES-1

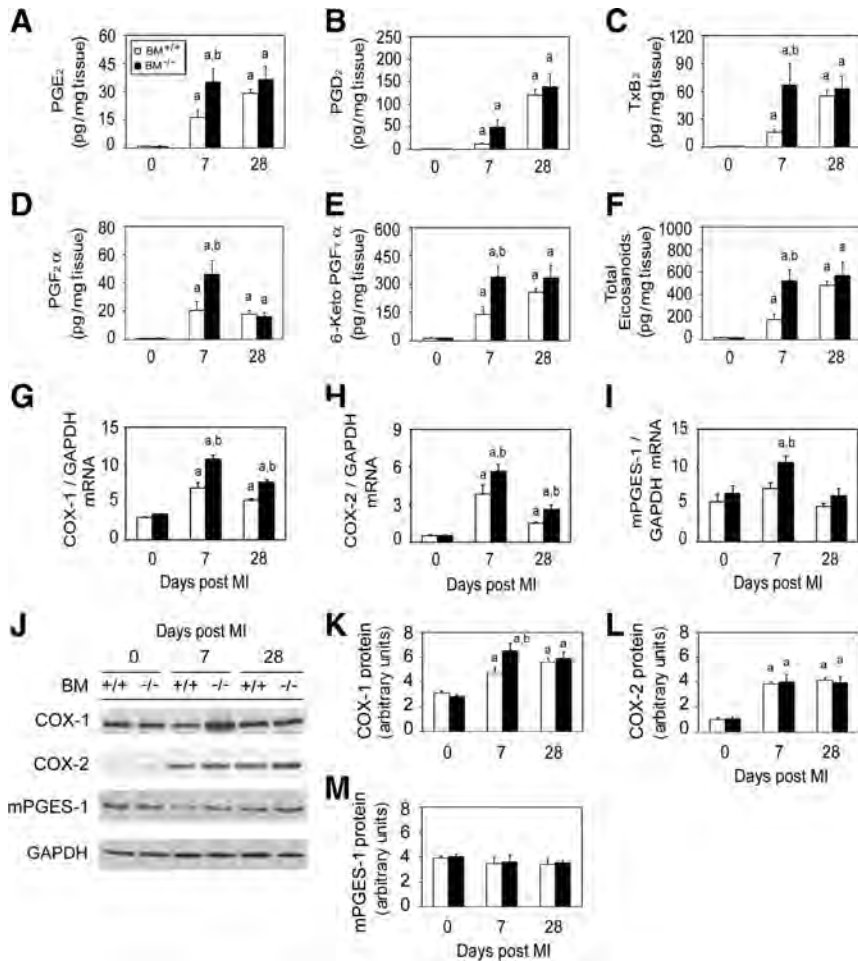


**Figure 3.** Lack of microsomal prostaglandin E<sub>2</sub> synthase-1 (mPGES-1) in myeloid cells leads to increased cyclooxygenase-1 (COX-1) expression and prostaglandin biosynthesis. Levels of prostaglandin E<sub>2</sub> (PGE<sub>2</sub>; **A**), PGD<sub>2</sub> (**B**), thromboxane B<sub>2</sub> (TxB<sub>2</sub>; **C**), PGF<sub>2α</sub> (**D**), 6 keto-PGF<sub>1α</sub> (**E**), and total prostaglandin levels (**F**; pg/mg of tissue) in the infarct, measured by liquid chromatography–tandem mass spectrometry before and 7 and 28 days after myocardial infarction (MI). Data represent  $\geq 12$  independent experiments per group. COX-1 (**G**), COX-2 (**H**), and mPGES-1 (**I**) mRNA levels in the infarct were measured by real-time polymerase chain reaction and normalized to GAPDH mRNA. Data represent  $\geq 6$  independent experiments for each group. **J**, Representative immunoblot analysis of COX-1, COX-2, mPGES-1, and GAPDH protein levels in the infarct in *BM*<sup>+/+</sup> and *BM*<sup>-/-</sup> mice after MI. Densitometric analysis of COX-1 (**K**), COX-2 (**L**), and mPGES-1 (**M**) protein. Open bars indicate *BM*<sup>+/+</sup> mice; solid bars, *BM*<sup>-/-</sup> mice. a,  $P < 0.05$  baseline vs 7 or 28 days after MI, *BM*<sup>+/+</sup> or *BM*<sup>-/-</sup> mice; b,  $P < 0.05$ , *BM*<sup>+/+</sup> vs *BM*<sup>-/-</sup> mice at any time point. Data represent  $\geq 6$  independent experiments for each group.

expression in the heart 7 days after MI, because that was when differences in prostaglandin levels in the infarct (Figures 3A through 3F) and LV (online-only Data Supplement Figure VI, A through F) were identified between *BM*<sup>-/-</sup> and *BM*<sup>+/+</sup> mice. Seven days after MI, COX-1 protein was present in the infarct, with apparently more intense staining in *BM*<sup>-/-</sup> than *BM*<sup>+/+</sup> mice (Figures 4A and 4B), consistent with the immunoblot analysis (Figures 3J and 3K). Scant cells stained positively for COX-2 protein 7 days after MI (Figures 4A and 4B). Inflammatory cells in the infarct zone expressed mPGES-1 protein in *BM*<sup>+/+</sup> mice (Figure 4A), as previously observed in *Ptges*<sup>+/+</sup> mice after MI.<sup>12</sup> In addition, elongated cells in the infarct zone of *BM*<sup>-/-</sup> mice also expressed mPGES-1 protein (Figure 4B). The identity of these cells is unknown, but they could not have been bone marrow-derived leukocytes, because all bone marrow-derived cells in *BM*<sup>-/-</sup> mice lacked the ability to express mPGES-1 (Figure 1A). Therefore, the cells that expressed mPGES-1 protein in *BM*<sup>-/-</sup> mice 7 days after MI must have been resident cardiac cells.

In contrast to the changes in prostaglandin biosynthetic enzyme gene expression in the infarcted myocardium (Figures 3G through 3I), there was no difference in COX-1, COX-2, mPGES-1, mPGES-2, or cPGES mRNA levels in the viable LV adjacent to the infarct in *BM*<sup>+/+</sup> and *BM*<sup>-/-</sup> mice after MI (online-only Data Supplement Figure VII, A through E).

### Cardiac Fibroblasts Express COX-1, COX-2, and mPGES-1 Protein in Infarcted Myocardium

To identify the resident cardiac cells that expressed mPGES-1 (Figure 4B) and COX-1 and COX-2 protein in the infarct of these chimeras, we performed multiple epitope ligand cartography–based evaluation of the LV of *Ptges*<sup>+/+</sup> and *Ptges*<sup>-/-</sup> mice and in *BM*<sup>+/+</sup> and *BM*<sup>-/-</sup> chimeras 7 days after MI (the time when differences in prostaglandin levels between *BM*<sup>+/+</sup> and *BM*<sup>-/-</sup> chimeras were noted; Figures 3A through 3F and online-only Data Supplement Figure VI, A through F). Multiple epitope ligand cartography enables sequential immunofluorescence-based visualization of multiple proteins in a tissue sample and can be used to identify the cell type that an individual protein is expressed in, and to determine which proteins colocalize in individual cells.<sup>19</sup>

In *Ptges*<sup>+/+</sup> mice, mPGES-1 localized with COX-1 and COX-2 in cardiac fibroblasts but was not expressed in cardiomyocytes after MI (online-only Data Supplement Figure VIII). As expected, there was no mPGES-1 staining in the LV of *Ptges*<sup>-/-</sup> mice, which served as a negative control, after MI (online-only Data Supplement Figure IX). In *BM*<sup>+/+</sup> chimeras, mPGES-1 colocalized with COX-1 and COX-2 in cardiac fibroblasts (Figures 4C through 4F; online-only Data Supplement Figure X). Because these cells also express PLA<sub>2</sub> enzymes,<sup>20</sup> cardiac fibroblasts have all of the enzymatic machinery necessary to catalyze PGE<sub>2</sub> biosynthesis. In con-

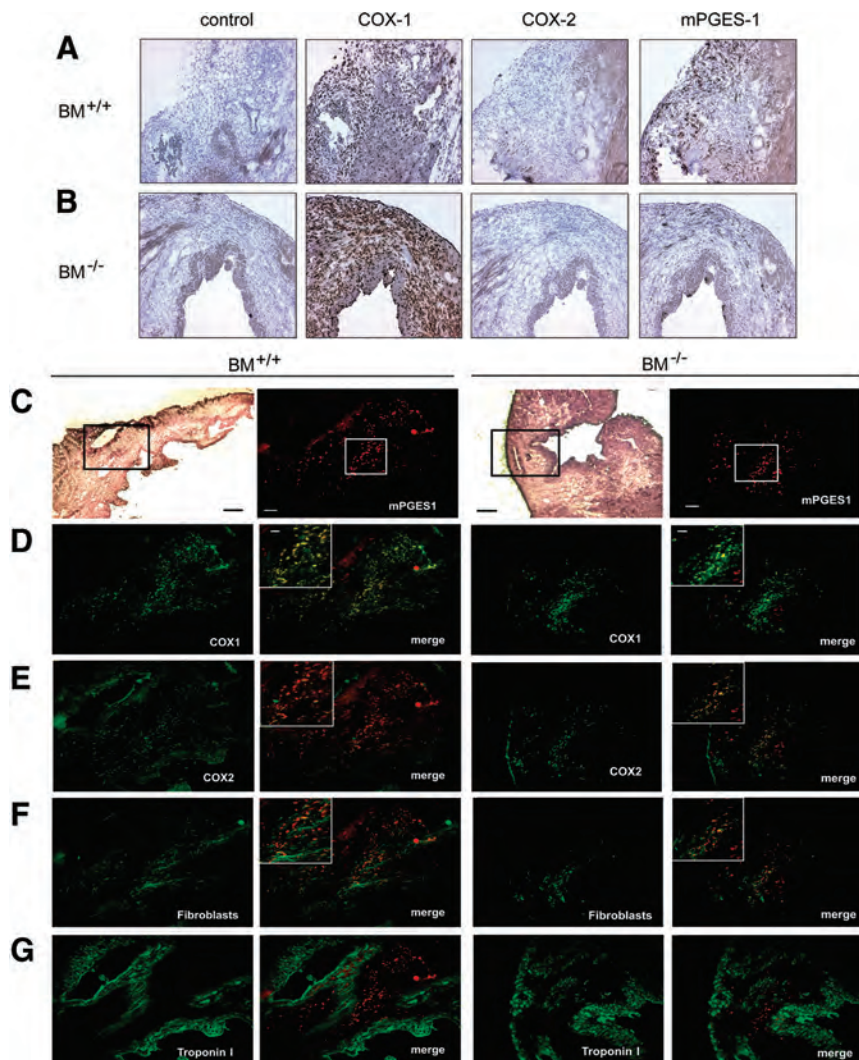


**Figure 4.** Microsomal prostaglandin E<sub>2</sub> synthase-1 (mPGES-1) colocalizes with cyclooxygenase-1 (COX-1) and COX-2 protein in cardiac fibroblasts after myocardial infarction (MI). Immunohistochemical analysis of COX-1, COX-2, and mPGES-1 in the LV 7 days after MI in *BM*<sup>+/+</sup> (A) and *BM*<sup>-/-</sup> (B) mice. Multiple epitope ligand cartography analysis of the expression of mPGES-1 (C), COX-1 (D), COX-2 (E), ER-TR7 (fibroblast marker; F), and troponin I (G) in *BM*<sup>+/+</sup> and *BM*<sup>-/-</sup> mice. In the second and fourth columns, the label “merge” identifies where mPGES-1 colocalized with COX-1, COX-2, ER-TR7, or troponin I. The area within the black rectangle in the Diff-Quick image for *BM*<sup>+/+</sup> and *BM*<sup>-/-</sup> mice is shown magnified in the mPGES-1, COX-1, COX-2, fibroblast, and troponin-1 images (magnification,  $\times 200$ ). The area within the white rectangle in the mPGES-1 image is shown magnified ( $\times 2$ ) in the upper left corner of the merged images for COX-1, COX-2, and fibroblasts. Scale bars: Diff-Quick, 200  $\mu$ m; mPGES-1, 50  $\mu$ m; white rectangle, 25  $\mu$ m. Images are representative of 5 independent studies.

trast, cardiomyocytes did not express mPGES-1 in *BM*<sup>+/+</sup> mice (Figure 4G) after MI. In *BM*<sup>-/-</sup> chimeras, mPGES-1 also colocalized with COX-1 and COX-2 in cardiac fibroblasts but did not colocalize with cardiomyocytes (Figures 4C through 4G; online-only Data Supplement Figure X). Taken together, these findings support the conclusion that the cells that stained positively for mPGES-1 on immunohistochemical analysis of *BM*<sup>-/-</sup> mice 7 days after MI (Figure 4B) were most likely cardiac fibroblasts.

#### Higher PGE<sub>2</sub> Production by Cardiac Fibroblasts Than Mononuclear Cells/Macrophages In Vitro

The relative capacity of cardiac fibroblasts and macrophages, the most prevalent inflammatory cell recruited to the infarct zone 7 days after MI,<sup>18</sup> to generate PGE<sub>2</sub> in vitro was evaluated next. Treatment with IL-1 $\beta$  increased PGE<sub>2</sub> production in vitro by bone marrow–derived mononuclear cells/macrophages and by cardiac fibroblasts from *Ptges*<sup>+/+</sup> mice (Figure 5A). On a per cell basis, cardiac fibroblasts produced 8.8-fold more PGE<sub>2</sub> than bone marrow–derived mononuclear cells/macrophages after exposure to IL-1 $\beta$  in vitro (Figure 5A). Although the protocol used generated a cellular population that was highly enriched in cardiac fibroblasts (online-

only Data Supplement Methods), it is possible that other cells in this preparation also produced PGE<sub>2</sub> in response to IL-1 $\beta$ .

Because PGH<sub>2</sub> generated by macrophages recruited to the infarct may diffuse out of these cells and be metabolized to PGE<sub>2</sub> by mPGES-1 in adjacent cardiac fibroblasts, we evaluated the effect of coculturing cardiac fibroblasts from *Ptges*<sup>+/+</sup> mice with mononuclear cells/macrophages from *Ptges*<sup>+/+</sup> or *Ptges*<sup>-/-</sup> mice in vitro. There is no difference in the level of PGE<sub>2</sub> in the supernatant of *Ptges*<sup>+/+</sup> cardiac fibroblasts after coculture with mononuclear cells/macrophages from either *Ptges*<sup>+/+</sup> or *Ptges*<sup>-/-</sup> mice and treatment with vehicle or IL-1 $\beta$  in vitro (Figure 5B).

#### Discussion

To the best of our knowledge, this is the first study to demonstrate that a prostaglandin biosynthetic enzyme in bone marrow–derived leukocytes, in this case mPGES-1, can regulate leukocyte infiltration, cardiomyocyte hypertrophy, LV systolic and diastolic function, and survival after MI. These findings are physiologically important because they suggest that mPGES-1 in bone marrow–derived leukocytes prevents pathological LV remodeling in a clinically relevant model of coronary artery occlusion in vivo.

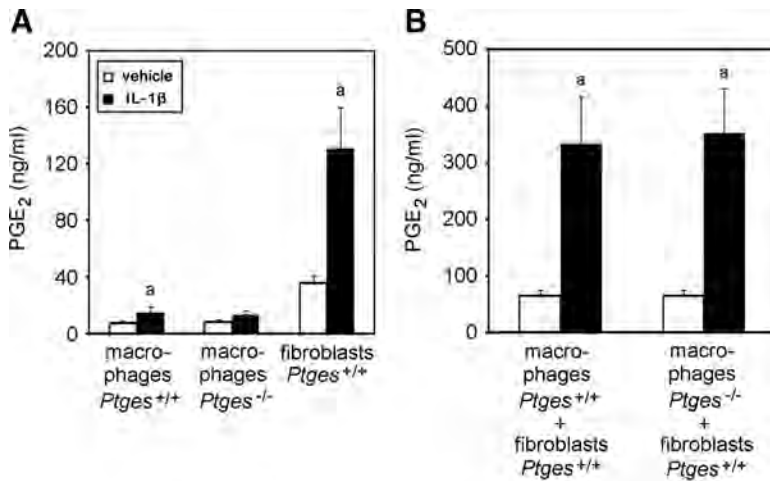


**Figure 5.** Higher prostaglandin E<sub>2</sub> (PGE<sub>2</sub>) production by cardiac fibroblasts than mononuclear cells/macrophages in vitro. Levels of PGE<sub>2</sub> in the supernatant of (A) cardiac fibroblasts ( $3 \times 10^4$ ) from *Ptges*<sup>+/+</sup> mice or mononuclear cells/macrophages ( $3 \times 10^4$ ) from *Ptges*<sup>+/+</sup> or *Ptges*<sup>-/-</sup> mice or (B) cardiac fibroblasts ( $3 \times 10^4$ ) from *Ptges*<sup>+/+</sup> mice cocultured with mononuclear cells/macrophages ( $1.5 \times 10^5$ ) from *Ptges*<sup>+/+</sup> or *Ptges*<sup>-/-</sup> mice. Open bars indicate vehicle; solid bars, interleukin-1β (IL-1β) 10 ng/mL. a,  $P < 0.05$  vehicle vs IL-1β. Data represent 4 independent experiments for each group, assayed in duplicate.

The molecular mechanism that leads to pathological LV remodeling in *BM*<sup>-/-</sup> compared with *BM*<sup>+/+</sup> mice may be related to the observation that levels of PGE<sub>2</sub> and other prostaglandins are higher in the viable LV adjacent to the infarct in *BM*<sup>-/-</sup> mice than in *BM*<sup>+/+</sup> mice. Importantly, there was no difference in the expression of prostaglandin biosynthetic enzymes in the viable LV adjacent to the infarct between these chimeras, so the differences in prostaglandin levels in the viable LV adjacent to the infarct cannot be explained by local differences in prostaglandin production. On the basis of these observations, we propose a novel model in which prostaglandins or their precursor PGH<sub>2</sub>, generated in the infarct, diffuse into the surrounding viable LV, interact with prostaglandin receptors on cardiomyocytes,<sup>4,10,21</sup> and act as paracrine regulators of cardiomyocyte hypertrophy and LV remodeling in vivo.

The present in vivo data do not permit identification of the prostaglandin(s) that modulate cardiac myocyte hypertrophy and pathological LV remodeling in *BM*<sup>-/-</sup> mice after MI. That limitation notwithstanding, the independent observations that (1) PGE<sub>2</sub> stimulates cardiac myocyte hypertrophy in vitro,<sup>4,10,22</sup> (2) inhibition or deletion of the PGE<sub>2</sub> receptor EP4 attenuates cardiomyocyte hypertrophy in vitro<sup>10</sup> and in vivo,<sup>21</sup> respectively, (3) *Ptges*<sup>-/-</sup> mice have lower levels of PGE<sub>2</sub> and less cardiac myocyte hypertrophy than *Ptges*<sup>+/+</sup> mice after MI,<sup>12</sup> (4) *Ptges*<sup>-/-</sup> mice have an impaired cardiac hypertrophic response compared with *Ptges*<sup>+/+</sup> mice to angiotensin II infusion in vivo,<sup>23</sup> and (5) *BM*<sup>-/-</sup> mice have higher levels of PGE<sub>2</sub> and more cardiac myocyte hypertrophy than *BM*<sup>+/+</sup> mice (cf Figures 1 and 3) strongly suggest that PGE<sub>2</sub> directly regulates cardiac myocyte hypertrophy after MI in vivo.

Independent molecular mechanisms may account for the increased levels of PGE<sub>2</sub> and other prostaglandins in the LV of *BM*<sup>-/-</sup> mice 7 days after MI. For example, COX-1 catalyzes the biosynthesis of PGH<sub>2</sub>, the precursor of all prostaglandins, and COX-1 mRNA and protein expression is higher in the infarct of *BM*<sup>-/-</sup> than *BM*<sup>+/+</sup> mice. Although inflammatory responses are commonly associated with increased COX-2 expression,<sup>24</sup> induction of COX-1 has been observed during inflammatory responses and cellular differentiation.<sup>25,26</sup> It is possible that IL-1β stimulates COX-1

expression in *BM*<sup>-/-</sup> mice after MI, because IL-1β can stimulate COX-1 expression in cultured fibroblasts under certain conditions,<sup>27</sup> and coronary ligation leads to higher IL-1β mRNA levels in the infarct of *BM*<sup>-/-</sup> than *BM*<sup>+/+</sup> mice (Figure 2A). In addition, targeted deletion of COX-2 can lead to a compensatory increase in COX-1 expression in some biological systems,<sup>28,29</sup> so it is possible that lack of COX-2–mPGES-1–catalyzed PGE<sub>2</sub> biosynthesis leads to a compensatory increase in COX-1 expression in *BM*<sup>-/-</sup> mice.

Because mPGES-2 and cPGES can also catalyze the terminal step in PGE<sub>2</sub> biosynthesis, the increase in PGE<sub>2</sub> levels in the heart of *BM*<sup>-/-</sup> mice could be catalyzed by COX-1–mPGES-2– or COX-1–cPGES–mediated pathways. Alternatively, cardiac fibroblasts, which express COX-1, COX-2, and mPGES-1 (Figure 4) and make ≈8.8-fold more PGE<sub>2</sub> on a per cell basis than mononuclear cells/macrophages in vitro after treatment with IL-1β (cf Figure 5A), may be a direct source of PGE<sub>2</sub> production in the heart after MI. A third possibility is that in inflammatory leukocytes recruited to the heart of *BM*<sup>-/-</sup> chimeras after MI, PGH<sub>2</sub> catalyzed by COX-1 or COX-2 builds up in these cells, because it is not metabolized by mPGES-1. This excess PGH<sub>2</sub> may diffuse out of inflammatory leukocytes and be metabolized to PGE<sub>2</sub> by mPGES-1 in adjacent cardiac fibroblasts. Although transcellular prostaglandin metabolism has been observed in other biological systems<sup>30</sup> and could explain the increase in PGE<sub>2</sub> levels in the infarct of *BM*<sup>-/-</sup> compared with *BM*<sup>+/+</sup> mice after MI, our failure to observe differences in PGE<sub>2</sub> production when cardiac fibroblasts from *Ptges*<sup>+/+</sup> mice were cocultured with mononuclear cells/macrophages from *Ptges*<sup>+/+</sup> or *Ptges*<sup>-/-</sup> mice mitigates against this hypothesis. A limitation of the present study is that our in vivo and in vitro data do not permit us to clearly identify which specific molecular pathway(s) or cells regulate PGE<sub>2</sub> production in the LV after MI.

MI stimulates an inflammatory response that is characterized by the sequential recruitment of polymorphonuclear leukocytes, macrophages, and monocytes that are necessary to clear necrotic debris and to promote matrix deposition, granulation tissue formation, angiogenesis, and infarct healing.<sup>18</sup> In addition, leukocyte-mediated oxidation reactions play a critical role in LV remodeling after MI.<sup>16</sup> Perturbations



in the inflammatory response are known to impair the recovery of LV function after infarction.<sup>31,32</sup> The observation that lack of mPGES-1 in bone marrow–derived cells increases IL-1 $\beta$ , IL-1 $\beta$  receptor antagonist, and tumor necrosis factor- $\alpha$  mRNA expression and leukocyte recruitment to the infarct (cf Figure 2) may explain the adverse LV remodeling that we observed in *BM*<sup>-/-</sup> compared with *BM*<sup>+/+</sup> mice after MI.

Inhibition of COX-2 leads to an imbalance of prothrombotic prostaglandins (increased TxA<sub>2</sub>) and antithrombotic prostaglandins (decreased PGI<sub>2</sub>) that is proposed to increase the risk of MI and stroke<sup>33</sup> and to increase mortality after MI.<sup>34</sup> Deletion of mPGES-1, downstream from COX-2 in the inducible PGE<sub>2</sub> biosynthetic cascade, decreases brain ischemia-reperfusion injury,<sup>35</sup> plaque burden in fat-fed *Ptges*<sup>-/-</sup> low-density lipoprotein receptor–deficient (*LDLR*<sup>-/-</sup>) mice,<sup>36</sup> aortic aneurysm formation,<sup>37</sup> and DOCA-salt– and angiotensin II–induced hypertension,<sup>38</sup> as well as pain, fever, and inflammation in animal models of these diseases.<sup>13,39</sup> Conversely, global deletion of mPGES-1 does not disturb the balance between prothrombotic and antithrombotic prostaglandin production in vivo. On the basis of these results, pharmacological inhibitors of mPGES-1 are proposed as an alternative to inhibition of COX-2 in the management of patients with atherosclerosis, pain, and inflammatory diseases.<sup>40</sup> The present results suggest that mPGES-1 in bone marrow–derived leukocytes negatively regulates the intensity of the inflammatory response to infarction and is necessary for physiological LV remodeling and recovery of LV contractile function after MI. Importantly, the effects of deletion of *Ptges* in bone marrow–derived leukocytes on cardiac physiology in mice may not be observed after administration of pharmacological inhibitors of the *Ptges* gene product mPGES-1 in animal models of MI, or in patients. For example, 50% of mice lacking COX-2 develop diffuse cardiac fibrosis, but this finding is not observed in patients taking selective COX-2 inhibitors, possibly because of incomplete pharmacological inhibition of COX-2 in vivo. In addition, inhibition of COX-2 is cardioprotective in mice<sup>41</sup> but results in adverse LV remodeling and LV rupture in a porcine MI model.<sup>42</sup> These observations underscore the need for caution in extrapolating our findings in mice to humans and identify the need to confirm these results in clinically relevant MI models in larger animals.

### Acknowledgments

This study is dedicated to the memory of Shafie Fazel and Helmut Schmidt.

### Sources of Funding

This study was supported by Canadian Institutes of Health Research grants (53297 to Dr Rubin, 14795 to Drs Li and Fazel), Swedish Medical Research Council, Swedish Rheumatism Association, King Gustaf V 80 Years and Marianne and Marcus Wallenberg's Foundation and Karolinska Institutet (Dr Jakobsson), and Deutsche Forschungsgemeinschaft DFG (GE 695) and Excellence Cluster 147 Cardiopulmonary System (ECCPS, Dr Geisslinger). Dr Keating is the Gloria and Seymour Epstein Chair in Cell Therapy and Transplantation at University Health Network. Dr Rubin is a Wylie Scholar in Academic Vascular Surgery, Foundation for Accelerated

Vascular Research, San Francisco and the Peter Munk Cardiac Centre Medical Director Chair.

### Disclosures

None.

### References

- Lopez AD, Murray CC. The global burden of disease, 1990–2020. *Nat Med*. 1998;4:1241–1243.
- Sutton MG, Sharpe N. Left ventricular remodeling after myocardial infarction: pathophysiology and therapy. *Circulation*. 2000;101:2981–2988.
- Pfeffer MA, Braunwald E. Ventricular remodeling after myocardial infarction: experimental observations and clinical implications. *Circulation*. 1990;81:1161–1172.
- Mendez M, LaPointe MC. Trophic effects of the cyclooxygenase-2 product prostaglandin E<sub>2</sub> in cardiac myocytes. *Hypertension*. 2002;39:382–388.
- Tanioka T, Nakatani Y, Semmyo N, Murakami M, Kudo I. Molecular identification of cytosolic prostaglandin E<sub>2</sub> synthase that is functionally coupled with cyclooxygenase-1 in immediate prostaglandin E<sub>2</sub> biosynthesis. *J Biol Chem*. 2000;275:32775–32782.
- Jakobsson PJ, Thoren S, Morgenstern R, Samuelsson B. Identification of human prostaglandin E synthase: a microsomal, glutathione-dependent, inducible enzyme, constituting a potential novel drug target. *Proc Natl Acad Sci U S A*. 1999;96:7220–7225.
- Trebino CE, Eskra JD, Wachtmann TS, Perez JR, Carty TJ, Audoly LP. Redirection of eicosanoid metabolism in mPGES-1-deficient macrophages. *J Biol Chem*. 2005;280:16579–16585.
- Giannico G, Mendez M, LaPointe MC. Regulation of the membrane-localized prostaglandin E synthases mPGES-1 and mPGES-2 in cardiac myocytes and fibroblasts. *Am J Physiol Heart Circ Physiol*. 2005;288:H165–H174.
- Degousee N, Angoulvant D, Fazel S, Stefanski E, Saha S, Iliescu K, Lindsay TF, Fish JE, Marsden PA, Li RK, Audoly LP, Jakobsson PJ, Rubin BB. c-Jun N-terminal kinase-mediated stabilization of microsomal prostaglandin E<sub>2</sub> synthase-1 mRNA regulates delayed microsomal prostaglandin E<sub>2</sub> synthase-1 expression and prostaglandin E<sub>2</sub> biosynthesis by cardiomyocytes. *J Biol Chem*. 2006;281:16443–16452.
- Mendez M, LaPointe MC. PGE<sub>2</sub>-induced hypertrophy of cardiac myocytes involves EP4 receptor-dependent activation of p42/44 MAPK and EGFR transactivation. *Am J Physiol Heart Circ Physiol*. 2005;288:H2111–H2117.
- Xiao CY, Yuhki K, Hara A, Fujino T, Kuriyama S, Yamada T, Takayama K, Takahata O, Karibe H, Taniguchi T, Narumiya S, Ushikubi F. Prostaglandin E<sub>2</sub> protects the heart from ischemia-reperfusion injury via its receptor subtype EP4. *Circulation*. 2004;109:2462–2468.
- Degousee N, Fazel S, Angoulvant D, Stefanski E, Pawelzik SC, Korotkova M, Arab S, Liu P, Lindsay TF, Zhuo S, Butany J, Li RK, Audoly L, Schmidt R, Angioni C, Geisslinger G, Jakobsson PJ, Rubin BB. Microsomal prostaglandin E<sub>2</sub> synthase-1 deletion leads to adverse left ventricular remodeling after myocardial infarction. *Circulation*. 2008;117:1701–1710.
- Trebino CE, Stock JL, Gibbons CP, Naiman BM, Wachtmann TS, Umland JP, Pandher K, Lapointe JM, Saha S, Roach ML, Carter D, Thomas NA, Durtschi BA, McNeish JD, Hambor JE, Jakobsson PJ, Carty TJ, Perez JR, Audoly LP. Impaired inflammatory and pain responses in mice lacking an inducible prostaglandin E synthase. *Proc Natl Acad Sci U S A*. 2003;100:9044–9049.
- Degousee N, Martindale J, Stefanski E, Cieslak M, Lindsay TF, Fish JE, Marsden PA, Thuerauf DJ, Glembofski CC, Rubin BB. MAP kinase kinase 6-p38 MAP kinase signaling cascade regulates cyclooxygenase-2 expression in cardiac myocytes in vitro and in vivo. *Circ Res*. 2003;92:757–764.
- Schubert W, Bonnekoh B, Pommer AJ, Philipsen L, Bockelmann R, Malykh Y, Gollnick H, Friedenberger M, Bode M, Dress AW. Analyzing proteome topology and function by automated multidimensional fluorescence microscopy. *Nat Biotechnol*. 2006;24:1270–1278.
- Askari AT, Brennan ML, Zhou X, Drinko J, Morehead A, Thomas JD, Topol EJ, Hazen SL, Penn MS. Myeloperoxidase and plasminogen activator inhibitor 1 play a central role in ventricular remodeling after myocardial infarction. *J Exp Med*. 2003;197:615–624.

17. Nahrendorf M, Pittet MJ, Swirski FK. Monocytes: protagonists of infarct inflammation and repair after myocardial infarction. *Circulation*. 2010;121:2437–2445.
18. Nahrendorf M, Swirski FK, Aikawa E, Stangenberg L, Wurdinger T, Figueiredo JL, Libby P, Weissleder R, Pittet MJ. The healing myocardium sequentially mobilizes two monocyte subsets with divergent and complementary functions. *J Exp Med*. 2007;204:3037–3047.
19. Linke B, Pierre S, Coste O, Angioni C, Becker W, Maier TJ, Steinhilber D, Wittpoth C, Geisslinger G, Scholich K. Toponomics analysis of drug-induced changes in arachidonic acid-dependent signaling pathways during spinal nociceptive processing. *J Proteome Res*. 2009;8:4851–4859.
20. Colston JT, de la Rosa SD, Strader JR, Anderson MA, Freeman GL. H<sub>2</sub>O<sub>2</sub> activates Nox4 through PLA2-dependent arachidonic acid production in adult cardiac fibroblasts. *FEBS Lett*. 2005;579:2533–2540.
21. Qian JY, Harding P, Liu Y, Shesely E, Yang XP, LaPointe MC. Reduced cardiac remodeling and function in cardiac-specific EP4 receptor knockout mice with myocardial infarction. *Hypertension*. 2008;51:560–566.
22. He Q, Harding P, LaPointe MC. PKA, Rap1, ERK1/2, and p90RSK mediate PGE<sub>2</sub> and EP4 signaling in neonatal ventricular myocytes. *Am J Physiol Heart Circ Physiol*. 2010;298:H136–H143.
23. Harding P, Yang XP, He Q, LaPointe MC. Lack of microsomal prostaglandin E synthase-1 reduces cardiac function following angiotensin II infusion. *Am J Physiol Heart Circ Physiol*. 2011;300:H1053–H1061.
24. Rouzer CA, Marnett LJ. Cyclooxygenases: structural and functional insights. *J Lipid Res*. 2009;50(suppl):S29–S34.
25. Choi SH, Aid S, Bosetti F. The distinct roles of cyclooxygenase-1 and -2 in neuroinflammation: implications for translational research. *Trends Pharmacol Sci*. 2009;30:174–181.
26. Wallace JL, Bak A, McKnight W, Asfaha S, Sharkey KA, MacNaughton WK. Cyclooxygenase 1 contributes to inflammatory responses in rats and mice: implications for gastrointestinal toxicity. *Gastroenterology*. 1998;115:101–109.
27. Kang YJ, Mbonye UR, DeLong CJ, Wada M, Smith WL. Regulation of intracellular cyclooxygenase levels by gene transcription and protein degradation. *Prog Lipid Res*. 2007;46:108–125.
28. Choi SH, Langenbach R, Bosetti F. Cyclooxygenase-1 and -2 enzymes differentially regulate the brain upstream NF- $\kappa$ B pathway and downstream enzymes involved in prostaglandin biosynthesis. *J Neurochem*. 2006;98:801–811.
29. Bosetti F, Langenbach R, Weerasinghe GR. Prostaglandin E<sub>2</sub> and microsomal prostaglandin E synthase-2 expression are decreased in the cyclooxygenase-2-deficient mouse brain despite compensatory induction of cyclooxygenase-1 and Ca<sup>2+</sup>-dependent phospholipase A<sub>2</sub>. *J Neurochem*. 2004;91:1389–1397.
30. Sala A, Folco G, Murphy RC. Transcellular biosynthesis of eicosanoids. *Pharmacol Rep*. 2010;62:503–510.
31. Panizzi P, Swirski FK, Figueiredo JL, Waterman P, Sosnovik DE, Aikawa E, Libby P, Pittet M, Weissleder R, Nahrendorf M. Impaired infarct healing in atherosclerotic mice with Ly-6C(hi) monocytosis. *J Am Coll Cardiol*. 2010;55:1629–1638.
32. Frangogiannis NG, Smith CW, Entman ML. The inflammatory response in myocardial infarction. *Cardiovasc Res*. 2002;53:31–47.
33. Bombardier C, Laine L, Reicin A, Shapiro D, Burgos-Vargas R, Davis B, Day R, Ferraz MB, Hawkey CJ, Hochberg MC, Kvien TK, Schnitzer TJ. Comparison of upper gastrointestinal toxicity of rofecoxib and naproxen in patients with rheumatoid arthritis: VIGOR Study Group. *N Engl J Med*. 2000;343:1520–1528.
34. Gislason GH, Jacobsen S, Rasmussen JN, Rasmussen S, Buch P, Friberg J, Schramm TK, Abildstrom SZ, Kober L, Madsen M, Torp-Pedersen C. Risk of death or reinfarction associated with the use of selective cyclooxygenase-2 inhibitors and nonselective nonsteroidal antiinflammatory drugs after acute myocardial infarction. *Circulation*. 2006;113:2906–2913.
35. Ikeda-Matsuo Y, Ota A, Fukada T, Uematsu S, Akira S, Sasaki Y. Microsomal prostaglandin E synthase-1 is a critical factor of stroke-reperfusion injury. *Proc Natl Acad Sci U S A*. 2006;103:11790–11795.
36. Wang M, Zukas AM, Hui Y, Ricciotti E, Pure E, FitzGerald GA. Deletion of microsomal prostaglandin E synthase-1 augments prostacyclin and retards atherogenesis. *Proc Natl Acad Sci U S A*. 2006;103:14507–14512.
37. Wang M, Lee E, Song W, Ricciotti E, Rader DJ, Lawson JA, Pure E, FitzGerald GA. Microsomal prostaglandin E synthase-1 deletion suppresses oxidative stress and angiotensin II-induced abdominal aortic aneurysm formation. *Circulation*. 2008;117:1302–1309.
38. Jia Z, Guo X, Zhang H, Wang MH, Dong Z, Yang T. Microsomal prostaglandin synthase-1-derived prostaglandin E<sub>2</sub> protects against angiotensin II-induced hypertension via inhibition of oxidative stress. *Hypertension*. 2008;52:952–959.
39. Engblom D, Saha S, Engstrom L, Westman M, Audoly LP, Jakobsson PJ, Blomqvist A. Microsomal prostaglandin E synthase-1 is the central switch during immune-induced pyresis. *Nat Neurosci*. 2003;6:1137–1138.
40. Romanovsky AA, Vioxx, Celebrex, Bextra ... Do we have a new target for anti-inflammatory and antipyretic therapy? *Am J Physiol Regul Integr Comp Physiol*. 2005;288:R1098–R1099.
41. LaPointe MC, Mendez M, Leung A, Tao Z, Yang XP. Inhibition of cyclooxygenase-2 improves cardiac function after myocardial infarction in the mouse. *Am J Physiol Heart Circ Physiol*. 2004;286:H1416–H1424.
42. Timmers L, Sluijter JP, Verlaan CW, Steendijk P, Cramer MJ, Emons M, Srijder C, Grundeman PF, Sze SK, Hua L, Piek JJ, Borst C, Pasterkamp G, de Kleijn DP. Cyclooxygenase-2 inhibition increases mortality, enhances left ventricular remodeling, and impairs systolic function after myocardial infarction in the pig. *Circulation*. 2007;115:326–332.

### CLINICAL PERSPECTIVE

Millions of patients use nonsteroidal anti-inflammatory drugs (NSAIDs) to treat pain and inflammatory disorders. NSAIDs block the activity of cyclooxygenase-2 (COX-2), an enzyme that catalyzes the second of three steps in prostaglandin biosynthesis. Unfortunately, some COX-2 inhibitors are associated with an increased risk of myocardial infarction (MI) and stroke, possibly because of decreased production of antithrombotic eicosanoids, such as PGI<sub>2</sub>, combined with simultaneous unopposed production of prothrombotic thromboxane A<sub>2</sub>, an eicosanoid catalyzed via COX-1 in platelets. Microsomal prostaglandin E<sub>2</sub> synthase-1 (mPGES-1) is downstream from COX-2 in the inducible PGE<sub>2</sub> biosynthetic pathway. Inhibition or deletion of mPGES-1 decreases pain, fever and inflammation without increasing the propensity for thrombosis. Therefore, pharmacologic inhibitors of mPGES-1 may be a viable replacement for COX-2 inhibitors, and may not be associated with an increased risk of thrombotic cardiovascular events. We show that targeted deletion of mPGES-1 in bone marrow derived leukocytes that are recruited to the heart leads to left ventricular (LV) dilation, impaired LV systolic and diastolic function, adverse LV remodeling, and increased mortality after MI. These findings increase our understanding of the molecular events that control LV remodeling after MI, and demonstrate the importance of eicosanoid biosynthesis by inflammatory leukocytes in this process. However, caution is warranted in extrapolating the results of targeted deletion of mPGES-1 in bone marrow derived leukocytes in mice to the possible outcome of pharmacologic inhibition of mPGES-1 in clinical practice. Further studies, of mice and humans, are warranted to define the role of mPGES-1 in LV remodeling after MI.